Ab Initio Calculations on the Thermodynamic Properties of Azaspiropentanes

Ryan M. Richard and David W. Ball*

Department of Chemistry, Cleveland State University, 2121 Euclid Avenue, Cleveland, Ohio 44115

Received: September 14, 2007; In Final Form: October 18, 2007

Following our recent study on the usefulness of borospiropentanes as new potential high-energy materials, we propose a new series of substituted spiropentane molecules, the azaspiropentanes. Presented here are the results of our ab initio calculations at the MP2 and B3LYP levels of theory using the 6-311++G(d,p) basis set. Results include optimized structural parameters, enthalpies of formation, specific enthalpies of combustion, and proton affinities. Our results indicate that azaspiropentane gives off the most energy of any of the nitrogen-containing spiropentanes, as indicated by its specific enthalpy of combustion of −41 kJ g^{-1}; however, it does not give off as much energy as spiropentane itself, which gives off about 48 kJ g^{-1}.

Introduction

Research involving the search for and synthesis of new high-energy (HE) materials is an ongoing quest. There are many molecules that fall into this category, and analysis of their characteristics yields several trends in structure and chemistry. These trends include strained ring structures, molecules that are unstable with respect to their combustion products, and the inclusion of various nitrogen-containing functional groups, such as nitro, nitrato, and amine groups.[1] Other studies offer additional traits, such as using boron and aluminum, due to the stability of their combustion products.[2]

Previously, we studied boron-substituted derivatives of spiropentane.[3] Our results indicated that the inclusion of boron atoms caused the resulting molecules to give off more energy upon combustion than spiropentane itself. This result is a direct consequence of the extra strain energy created by the inclusion of boron atoms in the ring, along with the fact that boron is thermodynamically unstable with respect to its combustion products. This results in an increase in the amount of energy given off by each molecule of borospiropentane when compared to spiropentane.

As a follow-up study, we have decided to study the effects of substitution of one or more of the carbon atoms in spiropentane by nitrogen atoms to generate azaspiropentane, two isomers of diazaspiropentane, triazaspiropentane, and tetraazaspiropentane. The nitrogen atoms are sp^3 hybridized, and therefore, their inclusion is not expected to raise the ring strain energy significantly; however, their inclusion in spiropentane might be thought to increase the thermodynamic instability of the molecule with respect to its combustion products.

Each possible nitrogen atom substitution has four different groups attached to it, three of which are the same for each nitrogen atom substituted into any position: a lone electron pair; a hydrogen atom; a spiro carbon atom. This means that each nitrogen atom will be chiral. From organic chemistry and simple probability theory, it is known that the total number of stereoisomers possible is given by two raised to the number of nitrogen atoms in the molecule; however, not all of these stereoisomers need be considered, as some are meso compounds while others are enantiomeric pairs which share all the same physical properties except the way they rotate polarized light. As a result of meso compounds and enantiomers, the total amount of stereoisomers that need be considered drops considerably. We will name the enantiomers using the standard *R*/*S* nomenclature system.

Spiropentane has been the subject of numerous experimental studies of its various properties. Spiropentane can be synthesized by debromination of pentaerythrityl bromide with zinc dust, using acetamide as a solvent.[4] Its structure has been studied using electron diffraction,[5] X-ray crystallography,[6] and nuclear magnetic resonance spectroscopy (NMR).[7] The infrared spectrum of spiropentane[8] was recorded shortly after its structure was established by the electron diffraction study.

Various theoretical studies have been done on spiropentane with a recent one done in 2001 by Dodziuk et al.[9] The purpose of their study was to update the previous theoretical work by using larger basis sets and by accounting for electron correlation; they reported optimized structural parameters, vibrational frequencies, and absolute NMR shieldings of spiropentane. Nguyen et al.[10] calculated the enthalpy of formation for spiropentane and several related molecules using various reactions. They also reported vibrational frequencies at the B3LYP/6-311G(d,p) level of theory.

No previous research has been done on any of the azaspiropentanes considered in this study, but a benzene derivative of azaspiropentane has been synthesized. *N*-Phenylazaspiropentane has been synthesized by Conover[11] by photolysis of triazoline in ether using 310 nm light, and the structure was confirmed by NMR. This reaction may provide a useful starting point for anyone attempting to synthesize any of the molecules studied here.

Computational Details

All calculations were performed on a personal computer using the Gaussian 03 computational chemistry program.[12] Computational methods used were Becke 3-parameter exchange plus

* To whom correspondence should be addressed. E-mail: d.ball@csuohio.edu.

10.1021/jp077411n CCC: $40.75
Published on Web 03/01/2008

the Lee, Yang, and Parr (B3LYP) correlation hybrid functional[13,14] and second-order Møller−Plesset (MP2) perturbation theory.[15−19] For both levels of theory, we used the 6-311G-(d,p) basis set[20] with diffuse functions on heavy atoms and hydrogen atoms.[21] The resulting structures and vibrations were visualized using GaussView, version 3.09.[22] Vibrational spectra were created using the SWizard program.[23]

In our previous study on spiropentane and its boron-containing derivatives,[3] we calculated the enthalpy of formation of spiropentane using a reaction previously proposed by Nguyen et al.,[10] which we list here as reaction 1:

$$C_5H_8(g) + CH_4(g) \rightarrow 2C_3H_6(g) \quad (1)$$

By taking the negative of the enthalpy of reaction of reaction 1 and correcting for the formation of the gaseous molecules using the enthalpies of formation obtained from the NIST Webbook website,[24] one obtains the enthalpy of formation for spiropentane. Similar reactions exist that allow the enthalpy of formation for the molecules considered in this study to be determined, as follows:

$$NC_4H_7(g) + CH_4(g) \rightarrow NC_2H_5(g) + C_3H_6(g) \quad (2)$$

$$N_2C_3H_6(g) + CH_4(g) \rightarrow C_3H_6(g) + N_2CH_4(g) \quad (3)$$

$$N_2C_3H_6(g) + CH_4(g) \rightarrow 2NC_2H_5(g) \quad (4)$$

$$N_3C_2H_5(g) + CH_4(g) \rightarrow N_2CH_4(g) + NC_2H_5(g) \quad (5)$$

$$N_4CH_4(g) + CH_4 \rightarrow 2N_2CH_4(g) \quad (6)$$

The enthalpies of formation for methane and cyclopropane were again taken from the NIST Webbook website.[24] The enthalpy of formation for azacyclopropane, NC_2H_5, is 126.8 kJ mol^{-1} according to Redley et al.[25] The enthalpy of formation of *trans*-diazacyclopropane, N_2CH_4, is 252.7 kJ mol^{-1} as reported by Alcami et al.[26] They did not report an enthalpy of formation value for *cis*-diazacyclopropane, nor were we able to locate one in the literature. Using the enthalpy of formation of the trans isomer, where the enthalpy of formation for the cis isomer should be used, is expected to lower the calculated enthalpy of formation slightly, as determined using reactions 3 and 5 above.

Once the enthalpy of formation of each azaspiropentane has been calculated, it is possible to calculate the enthalpy of combustion for each molecule using the general reaction listed as reaction 7:

$$N_xC_yH_z(g) + (9 + 0.5x)O_2(g) \rightarrow (0.5x)N_2(g) + yCO_2(g) + (0.5z)H_2O(\ell) \quad (7)$$

where

$$y(x) = 5 + x \quad (8)$$

$$z(x) = 8 - x \quad (9)$$

Reaction 7 and eqs 8 and 9 indicate that the enthalpy of combustion is proportional to the number of nitrogen atoms in the molecule, which we have defined as the variable "*x*". The enthalpies of formation for the combustion products were taken from the NIST Webbook website.[24] By dividing the enthalpy of combustion, obtained using reaction 7, by the molar mass of the molecule, one obtains the specific enthalpy of formation.

TABLE 1: Optimized Structural Parameters for Spiropentane and Associated Errors (Bond Lengths in Å; All Angles in deg; Errors in Percent)

param	B3LYP	MP2	exptl[5,6]	error
$r(C_t-H)$	1.085	1.085	1.08	0.5
$r(C_t-C)$	1.483	1.482	1.482	0.1
			1.48 ± 0.03	0.2
$r(C_t-C_t)$	1.531	1.532	1.527	0.3
			1.51 ± 0.04	1.5
$\alpha(H-C_t-H)$	114.6	115.5	120 ± 8	4.1
			115.0 ± 0.7	0.1
$\alpha(H-C_t-C_t)$	117.6	117.2		
$\alpha(H-C_t-C)$	118.5	118.2		
$\alpha(C_t-C-C_t)$	62.2	62.3	62.2	0.2
			61.5 ± 2	1.3
$\alpha(C_t-C_t-C)$	58.9	58.9		
$\delta(C_t-C_t-C-C_t)$	130.7	130.5		
$\delta(C-C_t-C_t-H)$	108.3	108.1		

The proton affinity (PA) is a fundamental measure of a molecule's Lewis base strength and is defined as the negative of the enthalpy of reaction of the protonation reaction. In determining the PA, we have used the protonation reaction listed here as reaction 10:

$$X(g) + H^+(g) \rightarrow XH^+(g) \quad PA \equiv -\Delta H_{rxn} \quad (10)$$

The symbol "X" in reaction 10 refers to the azaspiropentane of interest. When using reaction 10, we assumed that one of the nitrogen atoms was the site of the attack; this means that most of the molecules will have several different PAs, because of their chemically different nitrogen atoms.

Results and Discussion

Optimized Geometries. The optimized structural parameters for spiropentane are listed in Table 1 along with available experimental data. Data for the MP2 calculation were taken from our previous study of boraspiropentanes,[3] and it should be noted that the MP2 method used in that study is slightly different from the one we used for the azaspiropentanes in this study. In our previous study, we included the core electrons explicitly in the MP2 calculation by appending the MP2 keyword with the "full" keyword. This modification to the wave function had negligible effects on our previous data when compared to results predicted without including the core electrons explicitly, and thus, we chose not to include the core electrons explicitly in this study in an effort to reduce computation time. The optimized geometry for spiropentane is shown in Figure 1.

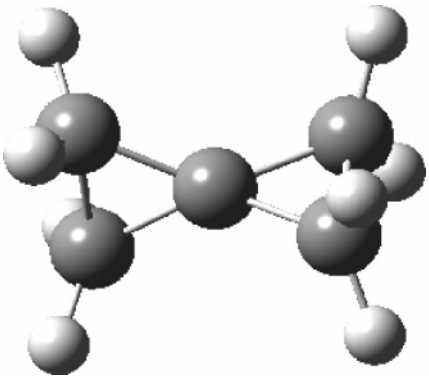

Figure 1. Optimized geometry for spiropentane. See Table 1 for structural parameters.

TABLE 2: Optimized Structural Parameters for Azaspiropentane (Bond Lengths in Å; Angles in deg)

param	B3LYP	MP2
r(N−H)	1.018	1.021
r(N−C_N)	1.499	1.507
r(N−C)	1.447	1.451
r(C_N−H)	1.086	1.086
r(C_N−C)	1.462	1.462
r(C−C_t)	1.480	1.481
r(C_t−C_t)	1.541	1.545
r(C_t−H)	1.085	1.085
α(H−N−C)	110.0	108.7
α(H−N−C_N)	110.0	107.8
α(N−C−C_N)	62.0	62.3
α(C−N−C_N)	59.5	59.2
α(H−C_N−H)	115.2	116.2
α(C_N−C−C_t)	139.7	139.7
α(C−C_t−H)	119.1	118.9
α(C−C_t−C_t)	58.7	58.4
δ(N−C_N−C−C_t)	127.8	127.5

TABLE 3: Optimized Structural Parameters for 1,2-Diazaspiropentane (Bond Lengths in Å; Angles in deg)

	stereoisomer			
	R,S		*R,R*	
param	B3LYP	MP2	B3LYP	MP2
r(H−N)	1.023	1.025	1.021	1.022
r(N−N)	1.539	1.550	1.530	1.542
r(N−C)	1.427	1.428	1.425	1.427
r(C−C_t)	1.479	1.479	1.474	1.473
r(C_t−H)	1.085	1.086	1.084	1.085
r(C_t−C_t)	1.549	1.554	1.549	1.554
α(H−N−N)	107.7	106.8	103.4	102.3
α(H−N−C)	108.2	107.0	108.9	107.6
α(N−N−C)	57.4	57.2	57.5	57.3
α(N−C−C_t)	134.2	134.0	134.3	134.0
α(C−C_t−H)	118.8	118.5	118.3	118.0
α(C−C_t−C_t)	58.6	57.8	58.3	58.2
α(H−C_t−H)	114.8	115.8	115.1	116.0
δ(N−N−C−C_t)	133.8	133.8	129.1	129.2

Tables 2−6 contain the optimized structural parameters for the azaspiropentane molecules involved in this study; the corresponding optimized geometries are depicted in Figures 2−8. The subscript "t" in these tables is for terminal, which is used to distinguish the terminal carbon atom from the spiro carbon atom. In Table 5 the prime notation is used to distinguish the nitrogen atom that is located next to the terminal carbon from the other two nitrogen atoms. The terminal carbon atoms that are located next to a nitrogen atom have the subscript "N" to distinguish them from the rest of the terminal carbon atoms. As mentioned previously, each isomer has several stereoisomers, and we have only listed the structural parameters for the unique diastereomers and meso compounds. In all cases, the enantiomers had structural parameters that were in excellent agreement with one another; the structural parameters of the enantiomers that did not match exactly usually matched to within 0.001 Å for bond distances and about 0.1° for angles.

In a comparison of the tables, there are several trends to note. First, the structural parameters of the stereoisomers do not differ too much among stereoisomers of the same molecule; this is to be expected and strengthens our confidence in our predicted values. The next point is that the MP2 level of theory in general predicts bond lengths that are longer than those predicted by the B3LYP level of theory. The differences between the two levels of theory are usually small, less than 0.01 Å for bond lengths and less than 1° for angles. We saw similar results in our previous study on boron-containing spiropentane derivatives.[3] Also worth mentioning is the value of the dihedral angle about the spiro carbon in the present study for each molecule, which is 125 ± 10°, depending on the molecule. Our previous study[3] had several molecules where this was not the case and in fact had dihedral angles that indicated that the spiro carbon was essentially planar; we explained this in terms of the empty p-orbital of the boron atom. The nitrogen atom does not have the ability to stabilize the planar geometry, as indicated by all of the minimum energy geometries having the two rings closer perpendicular to each other. We attribute the absence of perpendicularity to steric effects of the nitrogen lone electron pairs. For example, in the molecule hydrazine (NH_2NH_2) the minimum-energy geometry has the NH_2 groups staggered with respect to each other because of lone pair−lone pair repulsion. Hence, it comes as no surprise that none of the azaspiropentanes adopt a planar conformation like their boron-containing analogs.[3]

Vibrational Spectra. For comparison purposes, Table 7 lists the vibrational frequencies and infrared intensities calculated for spiropentane; the same caveat mentioned for Table 1, regarding the methodology, still applies. Again we refer to our previous study[3] for a more complete discussion.

Tables 8−12 list the vibrational frequencies, infrared intensities, and approximate mode descriptions for the most stable enantiomers for each formula as determined by their

TABLE 4: Optimized Structural Parameters for 1,4-Diazaspiropentane (Bond Lengths in Å; Angles in deg)

	stereoisomer					
	R,S		*R,R*		*S,S*	
param	B3LYP	MP2	B3LYP	MP2	B3LYP	MP2
r(N−H)	1.018	1.020	1.017	1.020	1.019	1.021
r(N−C_N)	1.509	1.517	1.505	1.514	1.512	1.520
r(N−C)	1.436	1.440	1.432	1.435	1.437	1.441
r(C_N−H)	1.086	1.089	1.086	1.086	1.084	1.084
r(C_N−C)	1.458	1.457	1.462	1.461	1.458	1.457
α(H−N−C_N)	110.2	109.0	110.6	109.2	109.2	107.8
α(H−N−C)	111.3	110.1	111.0	109.6	110.6	109.1
α(N−C_N−C)	57.6	57.9	57.7	57.7	57.9	57.9
α(H−C_N−H)	115.6	116.6	115.1	116.1	115.6	116.7
α(H−C_N−C)	118.9	118.6	119.0	118.7	120.9	120.5
α(C_N−C−C_N)	144.6	144.6	141.1	141.2	144.3	144.5
δ(N−C_N−C−N)	120.3	120.0	118.7	118.4	125.7	125.2

TABLE 5: Optimized Structural Parameters for Triazaspiropentane (Bond Lengths in Å; Angles in deg)

	stereoisomer							
	R,R,R		*R,R,S*		*R,S,R*		*S,R,S*	
param	B3LYP	MP2	B3LYP	MP2	B3LYP	MP2	B3LYP	MP2
r(N′−H)	1.018	1.020	1.017	1.020	1.017	1.020	1.018	1.020
r(N′−C)	1.420	1.424	1.421	1.424	1.414	1.416	1.427	1.431
r(N′−C_N)	1.515	1.524	1.515	1.525	1.510	1.519	1.521	1.529
r(C_N−H)	1.086	1.086	1.084	1.086	1.087	1.087	1.084	1.084
r(C_N−C)	1.457	1.456	1.458	1.457	1.463	1.462	1.453	1.451
r(C−N)	1.418	1.420	1.416	1.417	1.421	1.423	1.417	1.417
r(N−N)	1.541	1.556	1.543	1.557	1.547	1.561	1.554	1.568
r(N−H)	1.020	1.022	1.020	1.022	1.022	1.024	1.023	1.025
α(H−N′−C)	111.3	110.1	111.9	110.5	111.4	110.2	111.8	110.5
α(H−N′−C_N)	111.3	110.0	111.0	109.5	111.8	110.5	110.3	108.9
α(N′−C−C_N)	63.5	63.9	63.5	63.9	63.3	63.7	63.8	64.1
α(H−C_N−H)	115.7	116.6	115.7	116.6	115.2	116.2	116.1	116.9
α(H−C_N−C)	118.2	117.9	120.9	120.6	118.2	117.8	120.3	120.0
α(H−C_N−N′)	117.9	117.4	113.8	113.2	118.5	117.9	114.1	113.5
α(C−N−N)	57.0	56.6	57.2	56.9	56.9	56.6	56.9	56.6
α(C−N−H)	110.0	108.9	109.5	108.3	109.1	107.9	107.6	106.4
α(N−N−H)	103.9	102.7	104.0	102.8	108.5	107.3	107.8	107.0
δ(N′−C_N−C−N)	123.5	123.0	122.1	121.9	123.8	123.4	124.1	123.8

TABLE 6: Optimized Structural Parameters for Tetrazaspiropentane (Bond Lengths Are in Å, and Angles Are in Degrees)

	stereoisomer							
	R,R,R,R		*R,R,R,S*		*R,S,S,R*		*R,R,S,S*	
param	B3LYP	MP2	B3LYP	MP2	B3LYP	MP2	B3LYP	MP2
r(N−H)	1.021	1.022	1.021	1.022	1.023	1.025	1.020	1.022
r(N−N)	1.553	1.569	1.553	1.568	1.562	1.576	1.552	1.567
r(N−C)	1.410	1.411	1.403	1.404	1.405	1.406	1.407	1.409
α(H−N−N)	103.7	102.3	104.5	103.3	108.6	107.6	104.3	103.1
α(H−N−C)	109.9	108.6	109.3	108.2	108.5	107.3	109.7	108.5
α(N−N−C)	56.5	56.2	56.2	55.9	56.1	55.7	56.5	56.2
δ(N−N−C−N)	134.0	133.9	128.0	127.9	130.7	130.6	129.8	129.7

enthalpies of formation (Table 13). The predicted vibrational data for the remaining stereoisomers are available as Supporting Information. Figure 9 shows the vibrational spectra for these molecules using the vibrational frequencies and infrared intensities predicted by the B3LYP method. Azaspiropentane, *R,S*-1,2-diazaspiropentane, and *R,S,S*-triazaspiropentane all have C_1 symmetry. *R,R*-,1,2-Diazaspiropentane has C_2 symmetry, and

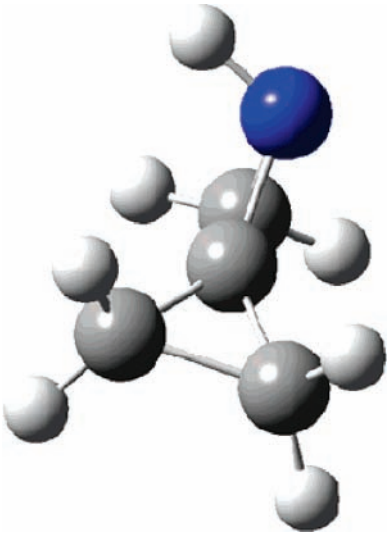

Figure 2. Optimized geometry for *R*-azaspiropentane. The enantiomer is *S*-azaspiropentane, which is not shown. Optimized structural parameters are located in Table 2.

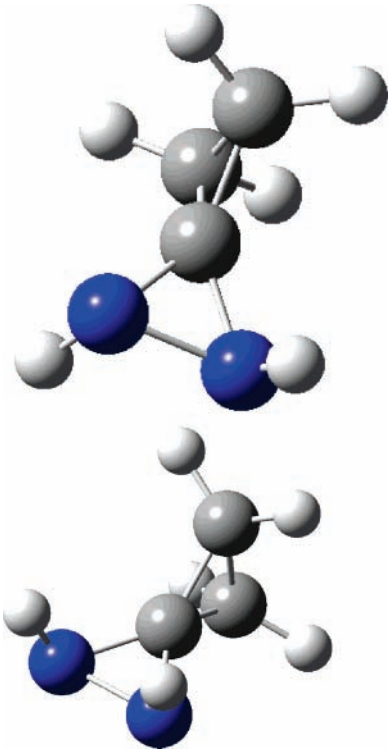

Figure 3. Optimized geometries of *R,R*-1,2-diazaspiropentane (top) and *R,S*-1,2-diazaspiropentane (bottom). See Table 3 for optimized structural parameters. The enantiomer is of the top molecule; *S,S*-1,2-diazaspiropentane, is not shown. The bottom molecule is a meso compound.

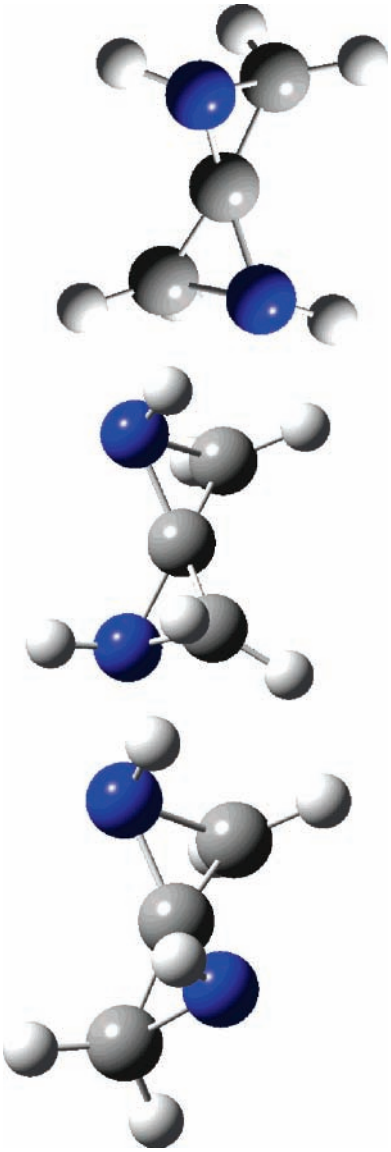

Figure 4. Optimized geometries of *R*,*R*-1,4-diazaspiropentane (top), *R*,*S*-1,4-diazaspiropentane (middle), and *S*,*S*-1,4-diazaspiropentane (bottom). See Table 4 for optimized structural parameters.

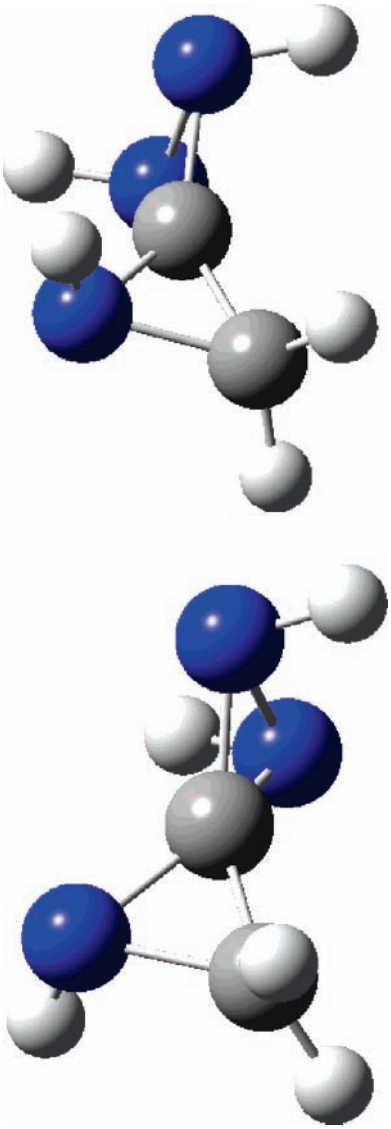

Figure 5. Optimized geometries for *R*,*R*,*R*-triazaspiropentane (top) and *R*,*R*,*S*-triazaspiropentane (bottom). See Table 5 for optimized structural parameters.

R,*R*,*S*,*S*-tetrazaspiropentane has S_4 symmetry. Thus, the vibrations transform as

$$\Gamma(\text{azaspiropentane}) = 30\ \text{A in}\ C_1$$

$$\Gamma(R,R\text{-1,2-diazaspiropentane}) = 14\ \text{A} + 13\ \text{B in}\ C_2$$

$$\Gamma(R,S\text{-1,4-diazaspiropentane}) = 24\ \text{A in}\ \text{C}_1$$

$$\Gamma(R,S,S\text{-triazaspiropentane}) = 21\ \text{A in}\ C_1$$

$$\Gamma(R,R,S,S\text{-tetrazaspiropentane}) = 5\ \text{A} + 6\ \text{B} + 5\ \text{E in}\ S_4$$

With the exception of the A mode in the S_4 point group, all modes are infrared active, indicating that the molecules should have 30, 27, 24, 21, and 11 (the E modes are doubly degenerate) infrared-active vibrations, respectively. This is in excellent agreement with our predicted results; any deviation can be attributed to not constraining the symmetry while optimizing the molecules.

Again, there are a couple of points to elucidate. The MP2 level of theory predicts vibrational frequencies that are in general higher than those predicted by the B3LYP level of theory; however, the MP2 level of theory tends to predict infrared intensities that are lower than those predicted by the B3LYP level of theory. In Table 12, the MP2 calculation predicts that *R*,*R*,*S*,*S*-tetrazaspiropentane will have two pairs of degenerate vibrations and three pairs of almost degenerate vibrations. The B3LYP method predicts that all five pairs will be almost degenerate. This difference most likely stems from not constraining the symmetry. In the same table, the MP2 level of theory predicts that the symmetric N−N stretch (561.8 cm^{-1}) will be infrared-inactive, but the B3LYP level of theory predicts that it will be slightly IR-active, with a predicted intensity of less than 0.1 km mol^{-1}.

With the exception of tetrazaspiropentane, the spectra in Figure 9 show remarkable similarity, and as a result, differentiating between the various molecules on the basis of IR spectra alone may be difficult. Figure 9 suggests that it should be possible to identify tetrazaspiropentane on the basis of its spectrum.

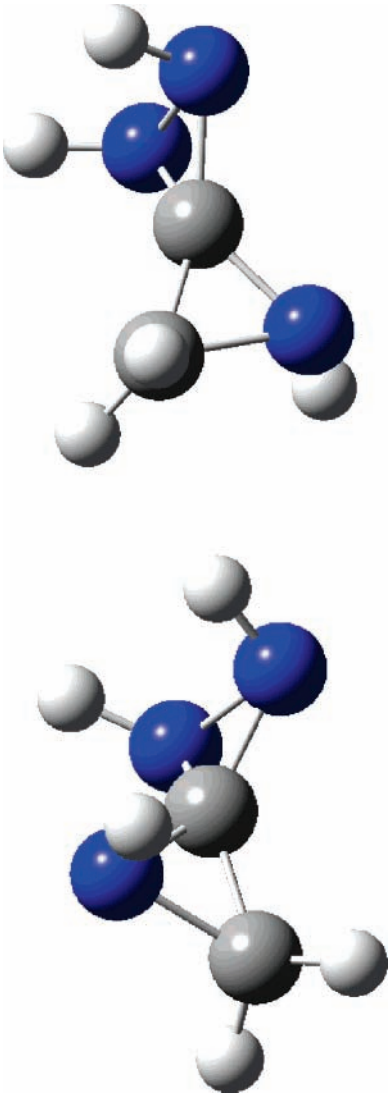

Figure 6. Optimized geometries for *R*,*S*,*R*-triazaspiropentane (top) and *S*,*R*,*R*-triazaspiropentane (bottom). Optimized structural parameters are listed in Table 5.

Enthalpies of Reaction. Table 13 lists the enthalpies of formation for spiropentane and its various azaspiropentane derivatives. Spiropentane is again included for comparison. The results obtained by our two methods are self-consistent; the MP2 level of theory tends to predict lower enthalpies of formation than the B3LYP level of theory by about 1 kJ mol^{-1}. Not surprising, spiropentane has the least positive enthalpy of formation, indicating that it is the thermodynamically most stable molecule. This validates our hypothesis that the substitution of the carbon atoms of spiropentane for nitrogen atoms will make the resulting molecule more thermodynamically unstable. The trend in enthalpies of formation for the nitrogen-containing derivatives is what is expected with the enthalpy of formation being directly proportional to the number of nitrogen atoms in the molecules.

The specific enthalpies of combustion for the studied molecules are located in Table 14. Because the two levels of theory agreed so well on the enthalpies of formation, it comes as no surprise that both predict the same specific enthalpies of combustion for each molecule. What is surprising is the trend in the ordering of the specific enthalpies of combustion, namely, that less energy is liberated/unit mass as the number

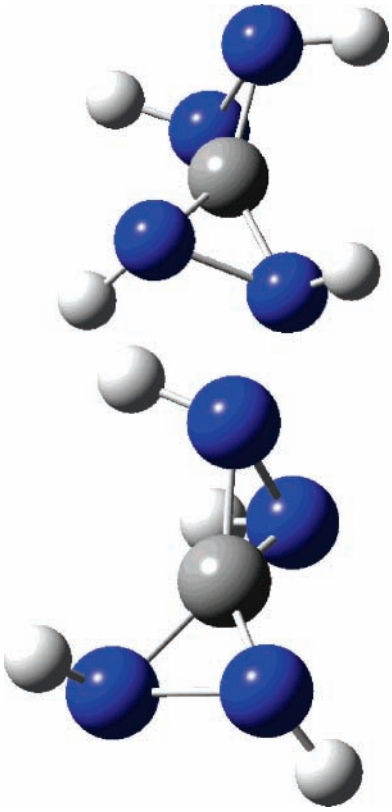

Figure 7. Optimized geometries of *R*,*R*,*R*,*R*-tetraazaspiropentane (top) and *R*,*S*,*S*,*S*-tetraazaspiropentane (bottom). See Table 6 for optimized structural parameters.

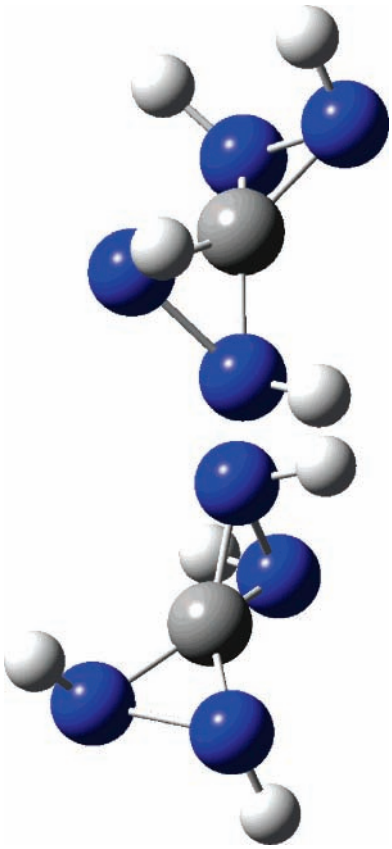

Figure 8. Optimized geometries for *R*,*S*,*S*,*R*-tetraazaspiropentane (top) and *R*,*R*,*S*,*S*-tetraazaspiropentane (bottom). See Table 6 for optimized structural parameters.

TABLE 7: Calculated Vibrational Frequencies, Infrared Intensities in Parentheses, and Approximate Descriptions for Spiropentane (Vibrational Frequencies in Wavenumbers; Infrared Intensities in km mol^{-1})

B3LYP	MP2	descriptn
292.1 (0.0)	297.0 (0.0)	ring twist
307.7 (0.2)	299.6 (0.2)	ring bend
598.1 (0.0)	610.4 (0.0)	ring stretch
788.1 (0.7)	800.2 (0.5)	CH_2 rock
842.0 (0.0)	852.8 (0.0)	CH_2 twist
884.1 (6.3)	911.7 (6.7)	CH_2 rock
884.1 (6.3)	911.8 (6.7)	CH_2 rock
890.5 (21.0)	917.6 (19.3)	C_t-C_t stretch
1009.1 (17.2)	1027.5 (19.9)	CH_2 wag
1023.0 (<0.1)	1036.9 (0.0)	CH_2 twist
1049.6 (0.0)	1070.0 (0.0)	CH_2 wag
1070.6 (<0.1)	1089.4 (0.0)	C_t-C_t stretch
1073.6 (1.6)	1077.8 (1.7)	CH_2 wag
1165.4 (0.0)	1181.0 (0.0)	CH_2 twist
1176.4 (0.1)	1191.5 (0.0)	CH_2 twist
1176.5 (1.7)	1198.4 (1.4)	CH_2 twist
1176.5 (1.6)	1198.5 (1.4)	CH_2 twist
1431.2 (<0.1)	1453.8 (<0.1)	sym CH_2 bend
1461.7 (1.7)	1476.0 (1.5)	asym CH_2 bend
1493.9 (0.0)	1510.1 (0.0)	asym CH_2 bend
1572.7 (0.5)	1621.3 (1.7)	sym CH_2 bend
3105.2 (28.2)	3165.8 (17.0)	asym C−H stretch
3105.2 (28.3)	3165.8 (17.0)	asym C−H stretch
3108.3 (39.2)	3171.4 (25.2)	sym C−H stretch
3109.2 (0.0)	3169.1 (0.0)	sym C−H stretch
3180.5 (0.0)	3258.7 (0.0)	asym C−H stretch
3181.7 (0.0)	3260.1 (0.0)	asym C−H stretch
3194.7 (25.2)	3272.0 (14.8)	asym C−H stretch

TABLE 8: Vibrational Frequencies, Infrared Intensities in Parentheses, and Approximate Descriptions for Azaspiropentane (Vibrational Frequencies in Wavenumbers; Infrared Intensities in km mol^{-1})

B3LYP	MP2	descriptn
297.1 (3.6)	299.2 (2.8)	ring twist
311.9 (1.2)	307.5 (2.0)	ring rock
362.6 (4.8)	362.3 (5.4)	ring rock
599.8 (2.7)	606.4 (2.4)	ring breathe
775.3 (3.1)	787.6 (2.5)	C_tH_2 twist
836.6 (46.4)	853.0 (43.6)	CH_2 twist
861.4 (7.1)	873.1 (2.2)	$N-C_N$ stretch
864.6 (12.8)	886.7 (14.4)	CH_2 rock
904.5 (11.3)	921.9 (12.6)	C_tH_2 twist
966.0 (16.6)	982.9 (16.3)	sym C_NH_2 rock + N−H rock
1027.0 (19.9)	1044.4 (12.8)	ring wag
1031.0 (5.4)	1066.8 (1.4)	CH_2 twist
1054.7 (1.4)	1049.3 (12.4)	CH_2 wag
1073.5 (1.2)	1082.2 (1.5)	C_tH_2 wag
1123.1 (6.3)	1138.3 (6.4)	C_NH_2 wag
1160.4 (9.9)	1181.1 (6.6)	CH_2 twist
1169.9 (0.1)	1186.4 (<0.1)	sym C_tH_2 twist
1239.6 (9.0)	1247.7 (6.5)	N−H wag
1255.4 (8.1)	1265.3 (6.5)	asym C_NH_2 rock + N−H rock
1442.2 (1.4)	1465.7 (0.7)	CH_2 bend
1453.6 (2.9)	1471.6 (2.4)	asym C_tH_2 bend
1493.7 (0.3)	1515.0 (0.2)	CH_2 bend
1585.5 (7.4)	1630.0 (4.2)	$CC_t + CC_N + C-N$ stretch
3097.3 (27.2)	3159.3 (15.1)	C_N-H stretch
3107.4 (19.3)	3162.9 (12.0)	asym C_tH_2 stretch
3114.5 (13.5)	3169.6 (8.5)	sym C_tH_2 stretch
3182.8 (14.4)	3259.5 (1.3)	asym C_N-H stretch
3186.5 (2.4)	3262.5 (8.2)	asym C_t-H stretch
3202.6 (15.9)	3274.0 (8.8)	sym C_t-H stretch
3475.9 (0.4)	3510.5 (1.4)	N−H stretch

TABLE 9: Vibrational Frequencies, Infrared Intensities in Parentheses, and Approximate Descriptions for *R,R*-1,2-Diazaspiropentane (Vibrational Frequencies in Wavenumbers; Infrared Intensities in km mol^{-1})

B3LYP	MP2	descriptn
322.0 (0.4)	309.2 (0.5)	ring rock
326.4 (1.1)	330.2 (1.3)	ring twist
397.3 (0.5)	396.6 (0.7)	ring rock
585.7 (1.6)	581.9 (1.1)	ring breathe
765.6 (0.9)	777.2 (0.5)	sym CH_2 rock
791.3 (4.3)	782.6 (3.8)	NN stretch
871.6 (24.4)	891.7 (24.3)	asym N−C stretch
885.4 (8.3)	896.2 (9.7)	asym CH_2 twist
931.6 (19.2)	948.8 (20.0)	N−H rock
1018.0 (0.6)	1026.0 (2.6)	C_t-C_t stretch
1030.4 (27.4)	1049.4 (26.5)	sym CH_2 wag
1074.6 (0.6)	1077.6 (36.3)	asym CH_2 wag
1109.9 (66.1)	1088.2 (29.9)	N−H wag
1165.2 (31.7)	1164.8 (55.8)	N−H rock
1172.9 (34.6)	1185.9 (0.7)	CH_2 twist
1182.8 (1.9)	1200.4 (2.4)	CH_2 twist
1306.7 (13.8)	1308.7 (6.8)	N−H rock
1340.4 (7.3)	1315.3 (10.6)	N−H wag
1447.6 (2.2)	1466.9 (1.3)	sym CH_2 bend
1449.9 (4.0)	1466.1 (3.5)	asym CH_2 bend
1585.8 (37.1)	1627.1 (27.5)	$N-C + CC_t$ stretch
3115.3 (14.2)	3168.5 (7.2)	asym CH_2 stretch
3117.6 (5.0)	3171.8 (2.5)	sym CH_2 stretch
3196.1 (<0.1)	3266.8 (<0.1)	asym C−H stretch
3208.4 (11.0)	3278.4 (5.3)	sym C−H stretch
3446.1 (0.4)	3486.6 (1.4)	sym N−H stretch
3452.8 (0.9)	3493.3 (3.4)	asym N−H stretch

TABLE 10: Vibrational Frequencies, Infrared Intensities in Parentheses, and Approximate Descriptions for *R,S*-1,4-Diazaspiropentane (Vibrational Frequencies in Wavenumbers; Infrared Intensities in km mol^{-1})

B3LYP	MP2	descriptn
307.1 (6.0)	308.7 (5.9)	ring twist
363.3 (1.7)	358.9 (1.9)	ring rock
392.5 (17.6)	393.3 (19.2)	ring rock
603.8 (6.3)	608.3 (5.4)	ring breathe
819.9 (66.8)	829.1 (45.5)	$N-C_N$ stretch
847.1 (24.7)	862.4 (35.3)	CH_2 twist
864.1 (36.0)	883.6 (36.6)	$C-N + CC_N$ stretch
943.2 (12.6)	951.2 (10.3)	CH_2 rock
946.9 (38.2)	962.4 (36.2)	CH_2 twist
961.6 (12.6)	973.2 (15.0)	CH_2 twist
1029.3 (29.1)	1037.5 (18.5)	CH_2 twist + CH_2 rock
1034.4 (1.0)	1047.0 (8.2)	CH_2 twist + CH_2 rock
1104.6 (6.2)	1120.0 (8.0)	CH_2 wag
1132.7 (12.7)	1147.7 (13.3)	CH_2 wag
1204.2 (12.6)	1215.6 (9.8)	N−H rock
1214.0 (16.7)	1224.3 (8.9)	N−H wag
1256.3 (11.3)	1265.7 (10.8)	N−H wag
1260.0 (5.1)	1268.7 (3.6)	N−H rock
1461.5 (4.6)	1486.0 (2.6)	asym CH_2 bend
1493.2 (0.3)	1515.1 (0.2)	sym CH_2 bend
1603.3 (38.4)	1648.2 (29.9)	$N-C + CC_N$ stretch
3096.2 (21.7)	3159.0 (12.2)	sym C−H stretch
3104.9 (20.2)	3166.5 (12.3)	sym C−H stretch
3182.1 (12.5)	3262.5 (6.7)	asym C−H stretch
3195.1 (9.6)	3273.4 (4.9)	asym C−H stretch
3483.1 (2.8)	3516.0 (5.6)	sym N−H stretch
3486.5 (1.3)	3522.3 (3.2)	asym N−H stretch

of nitrogen atoms increases. Ultimately, the explanation is simple: with each additional nitrogen atom, one less hydrogen atom is present and thus one-half less water molecule is produced upon combustion. The instability that results from the inclusion of the nitrogen atom does not compensate for this loss of energy given off when a water molecule is produced. The

TABLE 11: Vibrational Frequencies, Infrared Intensities in Parentheses, and Approximate Descriptions for *R,R,S*-Triazaspiropentane (Vibrational Frequencies in Wavenumbers; Infrared Intensities in km mol^{-1})

B3LYP	MP2	descriptn
326.9 (5.3)	327.6 (5.3)	ring twist
390.5 (3.7)	389.0 (4.6)	ring rock
428.1 (4.3)	424.2 (4.1)	ring rock
591.4 (2.2)	582.7 (1.6)	sym ring breathe
766.7 (23.4)	754.1 (16.1)	asym ring breathe
857.5 (57.7)	866.9 (71.4)	CH_2 twist
872.4 (74.4)	895.8 (62.5)	asym C−N stretch
946.8 (20.7)	955.9 (26.3)	CH_2 rock + N−H wag
970.2 (18.6)	970.8 (26.1)	N−H wag
1009.5 (28.1)	1002.3 (30.4)	C_N−N stretch
1102.8 (42.1)	1080.3 (44.1)	N−H wag
1120.8 (66.0)	1124.3 (58.3)	CH_2 wag + N−H wag
1154.7 (46.0)	1160.4 (21.5)	N−H rock
1175.1 (20.3)	1182.2 (18.6)	N−H rock
1237.7 (2.5)	1243.6 (2.9)	CH_2 rock + N−H wag
1315.3 (5.4)	1323.2 (3.4)	N−H rock
1325.8 (6.6)	1288.0 (6.7)	N−H wag
1471.1 (6.7)	1493.4 (4.4)	CH_2 bend
1598.3 (97.5)	1639.8 (81.7)	C−C_N + C−N stretch
3106.3 (13.8)	3167.7 (7.4)	sym C−H stretch
3196.2 (7.4)	3274.2 (3.5)	asym C−H stretch
3448.0 (1.7)	3487.9 (3.3)	sym N−H stretch
3459.9 (2.7)	3499.4 (5.6)	asym N−H stretch
3499.1 (4.3)	3530.5 (6.8)	N−H stretch

TABLE 12: Vibrational Frequencies, Infrared Intensities in Parentheses, and Approximate Descriptions for *R,R,S,S*-Tetrazaspiropentane (Vibrational Frequencies in Wavenumbers; Infrared Intensities in km mol^{-1})

B3LYP	MP2	descriptn
377.8 (9.1)	380.8 (10.0)	ring twist
424.8 (2.3)	420.6 (2.7)	ring rock
425.0 (2.3)	420.7 (2.7)	ring rock
573.0 (<0.1)	561.8 (0.0)	sym N−N stretch
722.9 (0.1)	697.5 (0.2)	asym N−N stretch
917.9 (56.6)	932.4 (56.9)	asym C−N stretch
918.1 (56.7)	932.5 (57.0)	asym C−N stretch
971.8 (<0.1)	955.2 (<0.1)	ring breathe
1093.0 (66.0)	1071.5 (66.7)	N−H wag
1093.6 (66.2)	1071.8 (66.9)	N−H rock
1099.5 (<0.1)	1096.2 (<0.1)	N−H rock
1142.1 (199.5)	1138.3 (184.9)	N−H rock
1290.4 (10.1)	1297.8 (8.7)	N−H rock
1290.6 (10.0)	1297.8 (8.7)	N−H rock
1317.1 (21.4)	1290.9 (18.1)	N−H wag
1318.3 (0.8)	1286.2 (<0.1)	N−H wag
1609.1 (171.3)	1644.9 (152.5)	C−N stretch
3460.2 (0.1)	3500.0 (<0.1)	sym N−H stretch
3463.0 (5.7)	3503.6 (9.0)	asym N−H stretch
3466.5 (12.2)	3507.1 (18.3)	asym N−H stretch
3467.2 (12.2)	3507.1 (18.3)	asym N−H stretch

predicted enthalpies of combustion in Table 14 indicate that spiropentane will give off the most energy/unit of mass when combusted, as indicated by its specific enthalpy of combustion of about −48 kJ g^{-1}. Azaspiropentane gives off the most energy of any of the nitrogen-containing compounds, as indicated by its specific enthalpy of combustion of about −41 kJ g^{-1}.

Using the enthalpy of formation for RDX (the main explosive component of the plastic explosive C4) obtained from the NIST Chemistry Webbook website,[24] one obtains a specific enthalpy of combustion of −7.4 kJ g^{-1}. This means that the molecules in this study give off about three to seven times more energy/unit of mass than RDX. The usefulness of these molecules as new HE materials will depend on their density, velocity of detonation, and cost to synthesize.

TABLE 13: Enthalpies of Formation (in kJ mol^{-1}) for Spiropentane and Its Nitrogen-Containing Derivatives

compd	B3LYP	MP2	exptl
spiropentane	183.5	180.4	185.1[24]
azaspiropentane	253.3	252.0	
R,R-1,2-diazaspiropentane	375.3	375.5	
R,S-1,2-diazaspiropentane	397.1	397.9	
R,R-1,4-diazaspiropentane	318.4	318.0	
R,S-1,4-diazaspiropentane	314.7	313.8	
S,S-1,4-diazaspiropentane	318.0	317.0	
R,R,R-triazaspiropentane	430.1	429.8	
R,R,S-triazaspiropentane	435.8	435.6	
R,S,R-triazaspiropentane	455.8	456.4	
S,R,R-triazaspiropentane	454.8	454.8	
R,R,R,R-tetrazaspiropentane	551.2	550.2	
R,R,R,S-tetrazaspiropentane	569.0	568.7	
R,S,S,R-tetrazaspiropentane	592.0	592.3	
R,R,S,S-tetrazaspiropentane	541.6	541.0	

TABLE 14: Specific Enthalpies of Combustion for Spiropentane and Its Nitrogen-Containing Derivatives (All Enthalpies in kJ g^{-1})

molecule	B3LYP	MP2
spiropentane	−48.4	−48.3
azaspiropentane	−40.9	−40.9
R,R-1,2-diazaspiropentane	−34.4	−34.4
R,S-1,2-diazaspiropentane	−34.7	−34.8
R,R-1,4-diazaspiropentane	−33.6	−33.6
R,S-1,4-diazaspiropentane	−33.6	−33.6
S,S-1,4-diazaspiropentane	−33.6	−33.6
R,R,R-triazaspiropentane	−27.2	−27.2
R,R,S-triazaspiropentane	−27.3	−27.3
R,S,R-triazaspiropentane	−27.5	−27.5
S,R,R-triazaspiropentane	−27.5	−27.5
R,R,R,R-tetrazaspiropentane	−21.0	−21.0
R,R,R,S-tetrazaspiropentane	−21.3	−21.3
R,S,S,R-tetrazaspiropentane	−21.6	−21.6
R,R,S,S-tetrazaspiropentane	−20.9	−20.9

Proton affinities as determined by the two methods used here are listed in Table 15; the columns indicate the nitrogen atom that was protonated. The message "same as X", where X is either 1 or 2, means that protonation at this nitrogen gives a structure that is the same as protonation at nitrogen X, and therefore, the PA will be the same. For comparison, ammonia, NH_3, has a PA of 851.4 kJ mol^{-1}.[27] This means that almost all of the azaspiropentane molecules will behave as bases and that most will be comparable in base strength to ammonia. One interesting trend to note regarding the data in Table 15 is that the MP2 level of theory predicts PA that are about 8 kJ mol^{-1} lower than those predicted by the B3LYP method in every case, suggesting that truncation at the second term may not be sufficient and higher order Møller−Plesset perturbation theory, such as MP4, may be required. It is also possible that the B3LYP level of theory is the lacking theory and consistently overestimates the PA by 8 kJ mol^{-1}. With no experimental PA available for these molecules, it is difficult to say which is the case or if it is a combination of both cases.

Conclusion

We have presented here ab initio calculations on the thermodynamic properties of mono-, di-, tri, and tetrasubstituted azaspiropentanes. Predicted properties include optimized struc-

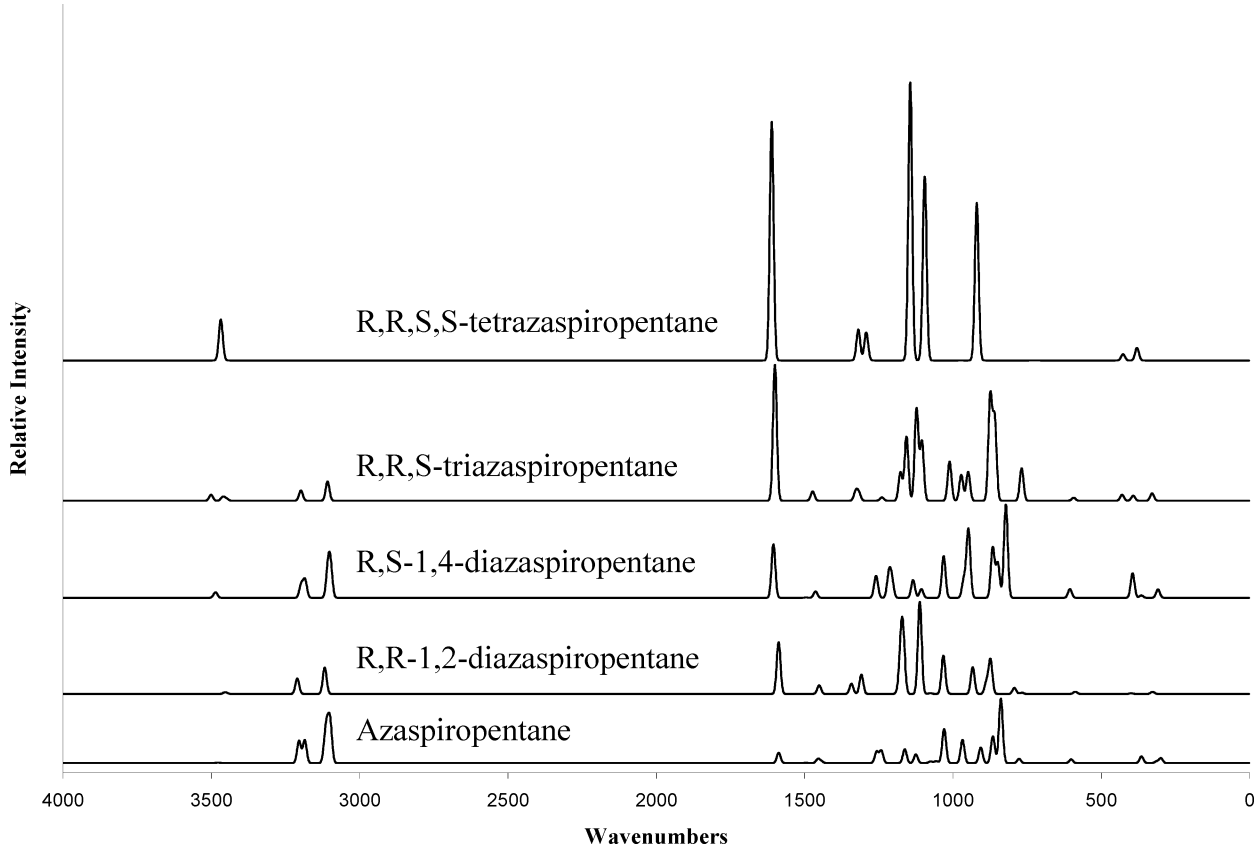

Figure 9. Vibrational spectra for the most stable conformers of the azaspiropentanes. All spectra are plotted to the same scale.

TABLE 15: Proton Affinities for the Various Azaspiropentanes (kJ mol^{-1})

	no. of nitrogen atoms							
	1		2		3		4	
molecule	B3LYP	MP2	B3LYP	MP2	B3LYP	MP2	B3LYP	MP2
azaspiropentane	925.3	918.4						
R,*R*-1,2-diazaspiropentane	870.3	860.9	same as 1					
R,*S*-1,2-diazaspiropentane	892.1	883.3	892.1	883.3				
R,*R*-1,4-diazaspiropentane	902.5	895.1	same as 1					
R,*S*-1,4-diazaspiropentane	913.2	905.7	898.8	890.8				
S,*S*-1,4-diazaspiropentane	916.5	908.9	same as 1					
R,*R*,*R*-triazaspiropentane	845.7	835.3	857.6	847.5	873.2	867.2		
R,*R*,*S*-triazaspiropentane	861.2	851.1	850.1	839.1	878.9	873.0		
R,*S*,*R*-triazaspiropentane	870.1	859.9	883.3	874.1	886.5	881.3		
S,*R*,*R*-triazaspiropentane	870.5	860.3	880.3	870.4	861.2	854.5		
R,*R*,*R*,*R*-tetrazaspiropentane	842.1	833.7	same as 1		same as 1		same as 1	
R,*R*,*R*,*S*-tetrazaspiropentane	828.4	820.3	same as 1		same as 1		842.1	833.7
R,*S*,*S*,*R*-tetrazaspiropentane	831.2	822.3	851.4	843.9	same as 2		same as 1	
R,*R*,*S*,*S*-tetrazaspiropentane	817.7	809.0	same as 1		same as 1		same as 1	

tural parameters, vibrational frequencies, infrared intensities, enthalpies of formation, specific enthalpies of combustion, and proton affinities. Our results indicate that spiropentane will give off the most energy when combusted, about 48 kJ g^{-1}, of the nitrogen-containing spiropentanes in this study; azaspiropentane gives off the most energy/gram, having a specific enthalpy of combustion of -41 kJ g^{-1}. The usefulness of any of these molecules as new potential high-energy materials will depend on their density, velocity of detonation, and cost to synthesize.

Acknowledgment. R.M.R. wishes to express gratitude to the Honors Program at Cleveland State University for its continued support.

Supporting Information Available: Tables of the vibrational frequencies of higher energy stereoisomers of di-, tri-, and tetrazaspiropentane. This material is available free of charge via the Internet at http://pubs.acs.org.

References and Notes

(1) Agrawal, J. P. *Prog. Energy Combust. Sci.* **1998**, *24*, 1.

(2) Politzer, P.; Lane, P.; Concha M. C. In *Chemistry at Extreme Conditions*; Manaa, M. R., Ed.; Elsevier: Amsterdam, 2005.

(3) Richard, R. M.; Ball, D. W. *J. Mol. Struct.*, accepted for publication.

(4) Murray, M. J.; Stevenson, E. H. *J. Am. Chem. Soc.* **1944**, *66*, 812.

(5) Donohue, J.; Humphrey, G. L.; Schomaker, V. *J. Am. Chem. Soc.* **1945**, *67*, 332.

(6) Boese, R.; Bläser, D.; Gomann, K.; Brinker, U. H. *J. Am. Chem. Soc.* **1989**, *111*, 1501.
(7) Bechtold, W.; Goldstein, J. H. *J. Am. Chem. Soc.* **1981**, *103* 4989.
(8) Cleveland, F. F.; Murray, M. J.; Gallaway, W. S. *J. Chem. Phys.* **1947**, *15*, 742.
(9) Dodziuk, H.; Leszczynski, J.; Jackowski, K. *Tetrahedron* **2001**, *57*, 5509.
(10) Nguyen, T. H.; Le, T. N.; Mebel, A. M.; Lin, S. H. *Chem. Phys. Lett.* **2000**, *326*, 468.
(11) Conover, W. W., II. Dissertation, Indiana University, Bloomingdale, IN, 1973.
(12) Frisch, M. J.; Trucks, G. W.; Schlegel, H. B.; Scuseria, G. E.; Robb, M. A.; Cheeseman, J. R.; Montgomery, J. A., Jr.; Vreven, T.; Kudin, K. N.; Burant, J. C.; Millam, J. M.; Iyengar, S. S.; Tomasi, J.; Barone, V.; Mennucci, B.; Cossi, M.; Scalmani, G.; Rega, N.; Petersson, G. A.; Nakatsuji, H.; Hada, M.; Ehara, M.; Toyota, K.; Fukuda, R.; Hasegawa, J.; Ishida, M.; Nakajima, T.; Honda, Y.; Kitao, O.; Nakai, H.; Klene, M.; Li, X.; Knox, J. E.; Hratchian, H. P.; Cross, J. B.; Bakken, V.; Adamo, C.; Jaramillo, J.; Gomperts, R.; Stratmann, R. E.; Yazyev, O.; Austin, A. J.; Cammi, R.; Pomelli, C.; Ochterski, J. W.; Ayala, P. Y.; Morokuma, K.; Voth, G. A.; Salvador, P.; Dannenberg, J. J.; Zakrzewski, V. G.; Dapprich, S.; Daniels, A. D.; Strain, M. C.; Farkas, O.; Malick, D. K.; Rabuck, A. D.; Raghavachari, K.; Foresman, J. B.; Ortiz, J. V.; Cui, Q.; Baboul, A. G.; Clifford, S.; Cioslowski, J.; Stefanov, B. B.; Liu, G.; Liashenko, A.; Piskorz, P.; Komaromi, I.; Martin, R. L.; Fox, D. J.; Keith, T.; Al-Laham, M. A.; Peng, C. Y.; Nanayakkara, A.; Challacombe, M.; Gill, P. M. W.; Johnson, B.; Chen, W.; Wong, M. W.; Gonzalez, C.; Pople, J. A. *Gaussian 03*, revision C.02; Gaussian, Inc.: Wallingford, CT, 2004.
(13) Lee, C.; Yang, W.; Parr, R. G. *Phys. Rev. B* **1988**, *37*, 785.
(14) Becke, A. D. *J. Chem. Phys.* **1993**, *98*, 5648.
(15) Head-Gordon, M.; Pople, J. A.; Frisch, M. J. *Chem. Phys. Lett.* **1988**, *153*, 503.
(16) Frisch, M. J.; Head-Gordon, M.; Pople, J. A. *Chem. Phys. Lett.* **1990**, *166*, 275.
(17) Frisch, M. J.; Head-Gordon, M.; Pople, J. A. *Chem. Phys. Lett.* **1990**, *166*, 281.
(18) Head-Gordon, M.; Head-Gordon, T. *Chem. Phys. Lett.* **1994**, *220*, 122.
(19) Saebo, S.; Almlof, J. *Chem. Phys. Lett.* **1989**, *154*, 83.
(20) Krishnan, R.; Binkley, J. S.; Seeger, R.; Pople, J. A. *J. Chem. Phys.* **1980**, *72*, 650.
(21) Clark, T.; Chandrasekhar, J.; Schleyer, P. v. R. *J. Comput. Chem.* **1983**, *4*, 294.
(22) Dennington, R., II; Keith, T.; Millam, J.; Eppinnett, K.; Hovell, W. L.; Gilliland, R. *GaussView*, version 3.09; Semichem, Inc.: Shawnee Mission, KS, 2003.
(23) Gorelsky, S. I. *SWizard program*, version 4.1; http://www.sg-chem.net/.
(24) *NIST Chemistry Webbook*; available at http://webbook.nist.gov/chemistry/; accessed July 28, 2007.
(25) Redley, J. B.; Naylor, R. D.; Kirby, S. P. *Thermochemical Data of Organic Compounds*; Chapmen and Hall: London, 1986.
(26) Alcami, M.; Mó, O.; Ýañez, M. *J. Comput. Chem.* **1988**, *19*, 1072.
(27) Szulejko, J. E.; McMahon, T. B. *J. Am. Chem. Soc.* **1993**, *115*, 7839.